

Third-order intrinsic anomalous Hall effect with generalized semiclassical theory

Longjun Xiang,¹ Chao Zhang,² Luyang Wang,¹ and Jian Wang^{1,3,*}

¹College of Physics and Optoelectronic Engineering, Shenzhen University, Shenzhen 518060, China

²Department of Physics, The Hong Kong University of Science and Technology, Clear Water Bay, Kowloon, Hong Kong, China

³Department of Physics, The University of Hong Kong, Pokfulam Road, Hong Kong, China

(Dated: January 31, 2023)

The linear intrinsic anomalous Hall effect (IAHE) and second-order IAHE have been intensively investigated in time-reversal broken systems. However, as one of the important members of the nonlinear Hall family, the investigation of third-order IAHE remains absent due to the lack of an appropriate theoretical approach, although the third-order extrinsic AHE has been studied within the framework of first- and second-order semiclassical theory. Herein, we generalize the semiclassical theory for Bloch electrons under the uniform electric field up to the third order using the wavepacket method and based on which we predict that the third-order IAHE can also occur in time-reversal broken systems. Same as the second-order IAHE, we find the band geometric quantity, the second-order field-dependent Berry curvature arising from the second-order field-induced *positional shift*, plays a pivotal role to observe this effect. Moreover, with symmetry analysis, we find that the third-order IAHE, as the leading contribution, is supported by 15 time-reversal broken 3D magnetic point groups (MPGs), corresponding to a wide class of antiferromagnetic (AFM) materials. Guided by the symmetry arguments, a two-band model is chosen to demonstrate the generalized theory. Furthermore, the generalized third-order semiclassical theory depends only on the properties of Bloch bands, implying that it can also be employed to explore the IAHE in realistic AFM materials, by combining with first-principles calculations.

Introduction.— As one of the important phenomena in condensed matter physics, the charge Hall effect and its variants, such as the anomalous Hall effect^{1,2} and spin Hall effect^{3,4}, have been studied continuously since its discovery in 1879⁵. For a long time, it has been believed that the observation of charge Hall current requires broken time-reversal (\mathcal{T}) symmetry⁶. However, within the framework of the first-order semiclassical theory⁷, Sodemann and Fu predicted⁸ that the second-order nonlinear Hall effect (NLHE) can exist even in \mathcal{T} -invariant materials, driven by the band geometric quantity Berry curvature dipole (BCD). Recently, this extrinsic (proportional to the relaxation time τ) NLHE has been observed experimentally^{9,10} and investigated theoretically^{11,12}.

In fact, slightly before investigating NLHEs within \mathcal{T} -invariant materials, the second-order nonlinear intrinsic (free of τ and depends only on the band topology) anomalous Hall effect (IAHE) in magnetic systems has been predicted by Y. Gao *et al.*¹³, by extending the semiclassical theory up to the second order. Very recently, with this second-order semiclassical theory, two research groups further predicted that the second-order nonlinear IAHE can be observed in \mathcal{PT} -symmetric compensated antiferromagnetic (AFM) materials CuMnAs¹⁴ and Mn₂Au¹⁵. Additionally, the intrinsic nonlinear planar Hall effects also have been proposed in magnetic Weyl semimetals¹⁶ and in nonmagnetic polar and chiral crystals¹⁷, respectively. Furthermore, using the second-order semiclassical theory, the extrinsic third-order NLHE has been investigated in materials^{18–22} with \mathcal{T} and \mathcal{P} symmetries, suggesting that the third-order Hall signal can be dominant in some materials. Besides, the extrinsic third-order nonlinear AHE, induced by Berry curvature quadrupole, can also be the leading contribution in some \mathcal{T} -broken ma-

terials, predicted by Zhang *et al.*²³ with the first-order semiclassical theory. However, as one of the important members of the nonlinear intrinsic anomalous Hall family, the third-order IAHE remains unexplored so far.

In this work, we generalize the semiclassical theory for Bloch electrons under the uniform electric field to third order using the wavepacket method and based on this we predict the existence of third-order IAHE in \mathcal{T} -broken systems. Like the second-order semiclassical theory¹³, we find the band geometric quantity, the second-order field dependent Berry curvature (BC) arising from the second-order field-induced *positional shift*¹³, plays a key role in observing this effect. Moreover, from symmetry analysis, we find that the third-order IAHE, as the leading contribution, can be hosted by 15 \mathcal{T} -broken 3D magnetic point groups (MPGs), corresponding to a wide class of AFM materials. Following the symmetry arguments, a two-band model is chosen to illustrate our generalized theory.

The third-order semiclassical theory.— Following the spirit of the semiclassical wavepacket approach^{7,13}, we focus on the 0th band (Throughout this work, we will only consider the Abelian case) and first construct the wavepacket¹³ as follows:

$$|\Psi\rangle = \int_{\mathbf{p}} e^{i\mathbf{p}\cdot\mathbf{r}} \left(C_0(\mathbf{p})|u_0(\mathbf{p})\rangle + \sum_{n \neq 0} C_n(\mathbf{p})|u_n(\mathbf{p})\rangle \right) \quad (1)$$

where $|u_n(\mathbf{p})\rangle$ is the Bloch state, C_0 is the zeroth-order amplitude with $|C_0|^2 = \delta(\mathbf{p} - \mathbf{p}_c)$ to normalize the wavepacket up to the first order⁷, $C_n = C_n^{(1)} + C_n^{(2)}$ with $C_n^{(1)}/C_n^{(2)}$ the first-order/second-order amplitude in

terms of the external electric field \mathbf{E} . Note that both $C_n^{(1)}$ and $C_n^{(2)}$ are related to C_0 , for example¹³,

$$C_n^{(1)} = \mathcal{M}_{n0} C_0 \quad (2)$$

where $\mathcal{M}_{n0} = \mathbf{E} \cdot \mathbf{A}_{n0} / (\epsilon_0 - \epsilon_n)$ with $\mathbf{A}_{n0} = \langle u_n | i\partial_{\mathbf{k}_c} | u_0 \rangle$ the interband Berry connection and $\epsilon_{0/n}$ the unperturbed band energy. Note that Eq.(2) is obtained by solving the time-dependent Schrödinger equation, therefore the relation between $C_n^{(2)}$ and C_0 can be identified similarly²⁴:

$$C_n^{(2)} = \left(\sum_{m \neq 0} \frac{\mathbf{E} \cdot \mathbf{A}_{nm} \mathcal{M}_{m0}}{\epsilon_0 - \epsilon_n} + \frac{\mathbf{E} \cdot i\partial_{\mathbf{p}} \mathcal{M}_{n0}}{\epsilon_0 - \epsilon_n} \right) C_0 + \frac{\mathbf{E} \cdot [(i\partial_{\mathbf{p}} - \mathbf{r}_c) C_0] \mathcal{M}_{n0}}{\epsilon_0 - \epsilon_n} \quad (3)$$

For the second order, we also must include a second-order correction $\frac{1}{2} \sum_{m \neq 0} \mathcal{M}_{0m} \mathcal{M}_{m0} C_0$ for C_0 in the first term of Eq.(1) to normalize the wavepacket up to the second order²⁵, which, together with Eq. (3), complete the construction of the second-order wavepacket.

Once the wavepacket is constructed, one can immediately calculate the wavepacket Lagrangian¹³ and then derive the equation of motion (EOM) describing the dynamics of the momentum (\mathbf{k}_c) and position (\mathbf{r}_c) centers of wavepacket under the uniform electric field ($e = \hbar = 1$):

$$\dot{\mathbf{r}}_c = \partial_{\mathbf{k}_c} \bar{\epsilon} - \dot{\mathbf{k}}_c \times \bar{\boldsymbol{\Omega}}, \quad (4)$$

$$\dot{\mathbf{k}}_c = -\mathbf{E}, \quad (5)$$

where $\partial_{\mathbf{k}_c} \equiv \partial / \partial \mathbf{k}_c$. Interestingly, we find that both the velocity and force equations keep the same form as the first- and second-order semiclassical EOM, but the band energy²⁵⁻²⁷ and Berry curvature¹³ in Eq.(4) should include the correction from the external electric field. Particularly, in Eq.(4), $\bar{\boldsymbol{\Omega}} \equiv \boldsymbol{\Omega} + \boldsymbol{\Omega}^{(1)} + \boldsymbol{\Omega}^{(2)}$ is the BC accurate to second order in terms of \mathbf{E} , where $\boldsymbol{\Omega}$ is the conventional BC and $\boldsymbol{\Omega}^{(1/2)}$ are the first- and second-order field-dependent BC, respectively. By calculating the first-order field-induced *positional shift* for the position center \mathbf{r}_c with the constructed wavepacket, Y. Gao *et al.*¹³ have successfully developed the second-order semiclassical theory. Herein, we further derive the second-order *positional shift* to generalize the semiclassical theory up to the third order.

Within the constructed wavepacket, the position center \mathbf{r}_c can be expressed as²⁸:

$$\mathbf{r}_c \equiv \langle \Psi | \mathbf{r} | \Psi \rangle = \partial_{\mathbf{k}_c} \gamma + \mathbf{A}_0 + \mathbf{A}_0^{(1)} + \mathbf{A}_0^{(2)} \quad (6)$$

where $\gamma = -\arg(C_0)$, $\mathbf{A}_0 = \langle u_0 | i\partial_{\mathbf{k}_c} | u_0 \rangle$ is the intra-band Berry connection, $\mathbf{A}_0^{(1)} = 2\text{Re} \sum_{n \neq 0} \mathbf{A}_{0n} \mathcal{M}_{n0}$ is the first-order *positional shift*, firstly derived by Y. Gao *et al.*¹³. At this stage, by taking the curl of \mathbf{A}_0 and $\mathbf{A}_0^{(1)}$, the conventional BC and the first-order field-dependent BC $\boldsymbol{\Omega}^{(1)}$ can be obtained and hence the first- and second-order semiclassical theories are formulated. Furthermore,

with the second-order wavepacket constructed in Eq.(1), we obtain the second-order *positional shift*²⁴:

$$\begin{aligned} \mathbf{A}_0^{(2)} = & \text{Re} \sum_{n \neq 0} \left[\frac{2\mathbf{A}_{0n} \mathbf{E} \cdot \mathbf{A}_{nm} \mathcal{M}_{m0}}{\epsilon_0 - \epsilon_n} - \mathcal{M}_{0n} \mathbf{A}_{nm} \mathcal{M}_{m0} \right] \\ & - \text{Re} \sum_{n \neq 0} \left[\frac{2\mathbf{E} \cdot \mathbf{A}_0 \mathcal{M}_{n0} \mathbf{A}_{0n}}{\epsilon_0 - \epsilon_n} - \mathbf{A}_0 \mathcal{M}_{0n} \mathcal{M}_{n0} \right] \\ & - \text{Re} \sum_{n \neq 0} \left[\mathcal{M}_{0n} i\partial_{\mathbf{k}_c} \mathcal{M}_{n0} - \frac{\mathbf{A}_{0n} \mathbf{E} \cdot i\partial_{\mathbf{k}_c} \mathcal{M}_{n0}}{\epsilon_0 - \epsilon_n} \right] \\ & - \text{Re} \sum_{n \neq 0} \mathcal{M}_{n0} \mathbf{E} \cdot i\partial_{\mathbf{k}_c} \left(\frac{\mathbf{A}_{0n}}{\epsilon_0 - \epsilon_n} \right) \end{aligned} \quad (7)$$

where we have replaced the momentum center \mathbf{p}_c with \mathbf{k}_c at the final results. Importantly, by defining $\mathcal{A}_0^{\alpha, (2)} \equiv T_{\alpha\beta\gamma}^0 E_\beta E_\gamma$ with $T_{\alpha\beta\gamma}^0$ the second-order *Berry-connection polarizability tensor* (BPT) for band 0, we find

$$T_{\alpha\beta\gamma}^0 = \text{Re} \sum_n \left(\mathcal{U}_{0n}^{\alpha\beta\gamma} + \mathcal{U}_{0n}^{\beta\alpha\gamma} - \mathcal{U}_{n0}^{\beta\gamma\alpha} - \sum_m \mathcal{V}_{0nm}^{\alpha\beta\gamma} \right) \quad (8)$$

with

$$\mathcal{U}_{0n}^{\alpha\beta\gamma} \equiv M_{0n}^\beta (\mathcal{A}_0^\alpha - \mathcal{A}_n^\alpha - i\partial_\alpha) M_{n0}^\gamma,$$

$$\mathcal{V}_{0nm}^{\alpha\beta\gamma} \equiv (2M_{0n}^\alpha \mathcal{A}_{nm}^\beta + M_{0n}^\beta \mathcal{A}_{nm}^\alpha) M_{m0}^\gamma \bar{\delta}_{nm},$$

where $\mathcal{A}_n^\alpha = \langle u_n | i\partial_\alpha | u_n \rangle$ with $\partial_\alpha \equiv \partial / \partial k_c^\alpha$ and $M_{mn}^\alpha = \mathcal{A}_{mn}^\alpha / (\epsilon_n - \epsilon_m) \bar{\delta}_{nm}$ with $\bar{\delta}_{nm} \equiv 1 - \delta_{nm}$. Interestingly, under $U(1)$ gauge transformation $|u_n\rangle \rightarrow e^{i\phi_n} |u_n\rangle$, we find that $\mathcal{A}_n^\alpha \rightarrow \mathcal{A}_n^\alpha - \partial_\alpha \phi_n$, $\mathcal{A}_{mn}^\alpha \rightarrow e^{i(\phi_n - \phi_m)} \mathcal{A}_{mn}^\alpha$, and $M_{mn}^\alpha \rightarrow e^{i(\phi_n - \phi_m)} M_{mn}^\alpha$, therefore, \mathcal{U} , \mathcal{V} , and T are $U(1)$ gauge invariant. Same as the physical implication of $\mathcal{A}_0^{(1)}$ ¹³, $\mathcal{A}_0^{(2)}$ stands for a second-order correction to the conventional Berry connection \mathbf{A}_0 of the unperturbed band, which means that the wavepacket also acquires a shift $\mathbf{A}_0^{(2)}$ in its center \mathbf{r}_c of mass position. In addition, we note that $\mathcal{A}_0^{(2)}$ also respects the periodicity of the lattice due to the uniform external field, hence it does not cause any macroscopic charge density gradient and also will not affect the electron chemical potential profile^{13,29}. The second-order BPT is the central concept of our third-order semiclassical theory.

By taking the curl of the second-order field-dependent Berry connection, we obtain the field-dependent BC $\boldsymbol{\Omega}^{(2)}$ at the same order. Furthermore, substituting $\boldsymbol{\Omega}^{(2)}$ into Eq.(4), the third-order semiclassical theory is established when the band energy $\bar{\epsilon}$ is corrected to third-order²⁴. Like the second-order semiclassical theory, the third-order EOM and the second-order field-dependent BC, plays an essential role in investigating the IAHE in AFM materials, as will be illustrated below, especially when the linear and second-order IAHE signals are forbidden by symmetry. The third-order semiclassical theory, with the second-order field-dependent BC originating from the

TABLE I. The classification for 90 \mathcal{T} -broken MPGs in 3D with the third-, and fourth-order IAHEs, as the leading contribution.

The order of IAHE	The MPGs for IAHE
Third-order	mmm , $4'/m$, $4/mmm$, $4'/mm'm$, $\bar{3}m$, $6'$, $6'/m'$, $6'22'$, $6'mm'$, $\bar{6}m2$, $6/mmm$, $6'/m'mm'$, $m\bar{3}$, $4'32'$, $m\bar{3}m'$
Fourth-order	$6'/m$, $6'/mmm'$, $\bar{4}3m$, $m'\bar{3}'m$

second-order field-induced *positional shift* as the band geometric quantity, is our first main result.

The third-order IAHE. — Within the framework of third-order semiclassical transport theory, if we ignore the scattering effects arising from impurities, the third-order intrinsic Hall current density can be expressed as $J_\alpha = \chi_{\alpha\beta\gamma\eta}^{\text{int}} E_\beta E_\gamma E_\eta$, where

$$\chi_{\alpha\beta\gamma\eta}^{\text{int}} = \int_k \Lambda_{\alpha\beta\gamma\eta} f_0 \quad (9)$$

is the third-order intrinsic Hall conductivity, which is a rank-4 tensor. In Eq.(9), f_0 is the equilibrium Fermi distribution function, and

$$\Lambda_{\alpha\beta\gamma\eta} = \sum_n [\partial_\beta T_{\alpha\gamma\eta}^n - \partial_\alpha T_{\beta\gamma\eta}^n] \quad (10)$$

is the integrand for the third-order intrinsic Hall conductivity, which is antisymmetric in its first two indices and symmetric in its last two indices, namely $\chi_{\alpha\beta\gamma\eta}^{\text{int}} = -\chi_{\beta\alpha\gamma\eta}^{\text{int}}$ and $\chi_{\alpha\beta\gamma\eta}^{\text{int}} = \chi_{\beta\alpha\eta\gamma}^{\text{int}}$. By performing an integration by parts for Eq.(9), we find that the third-order IAHE is also a Fermi liquid property^{8,13–15,30}, as expected.

Symmetry analysis. — Next, we investigate what kind of symmetry will host a non-vanishing third-order intrinsic Hall current and when this response becomes the leading contribution. It has been well known that the number of independent components of a physical quantity such as conductivity tensor is dictated by the magnetic point group (MPG) symmetry of the system, as required by Neumann's principle^{31,32}. Under \mathcal{T} -symmetry, the field dependent BC is \mathcal{T} -odd and hence there is no intrinsic Hall signal in \mathcal{T} -invariant systems. However, for materials with \mathcal{T} -broken MPGs, the BC is nonzero and hence we can observe the intrinsic Hall signal in these systems.

In particular, for the rank-4 IAHE conductivity tensor $\chi_{\alpha\beta\gamma\eta}^{\text{int}}$, the constraint imposed by MPG symmetry operations R and $R\mathcal{T}$ can be expressed as³²:

$$\chi_{\alpha\beta\gamma\eta}^{\text{int}} = \eta_T R_{\alpha\alpha'} R_{\beta\beta'} R_{\gamma\gamma'} R_{\eta\eta'} \chi_{\alpha'\beta'\gamma'\eta'}^{\text{int}} \quad (11)$$

where $\eta_T = 1$ ($\eta_T = -1$) is for $R(R\mathcal{T})$ and $R_{\alpha\alpha'}$ is the matrix element of the spatial point group operation R . Starting from Eq.(11), in principle we can classify the 90 3D MPGs without \mathcal{T} (ruled out 32 grey MPGs in total 122 MPGs in 3D) using the linear, second-order, third-order, and other high-order IAHEs. For example, considering the MPG $6'$ with the generator $C_6\mathcal{T}$, we find $\chi_{xxxx}^{\text{int}} = -\chi_{zzzz}^{\text{int}} = \chi_{xyxy}^{\text{int}} = -\chi_{xzyy}^{\text{int}} = -\chi_{yzxy}^{\text{int}} = -\chi_{zyyx}^{\text{int}} = \chi_{zyxy}^{\text{int}} = \chi_{zyyx}^{\text{int}} \neq 0$ and $\chi_{xxxy}^{\text{int}} = -\chi_{xyxx}^{\text{int}} = -\chi_{yzxx}^{\text{int}} = -\chi_{zyyy}^{\text{int}} = -\chi_{zyxx}^{\text{int}} = \chi_{zyyy}^{\text{int}} \neq 0$, whereas both the rank-2 and rank-3 conductivity tensors $\chi_{\alpha\beta}^{\text{int}}$ and $\chi_{\alpha\beta\gamma}^{\text{int}}$ vanish for linear IAHE and second-order IAHE, respectively.

On the other hand, we can also define Jahn's notations³³ $a\{V^2\}$, $a\{V^2\}V$, $a\{V^2\}[V^2]$ and $a\{V^2\}[V^3]$ for linear, second-order, third-order, and fourth-order IAHE conductivity tensors, respectively, and then use Bilbao Crystallographic Server³⁴ to find the 3D MPGs with a non-vanishing Hall signal²⁴ and identify the leading contribution, as shown in TABLE I. We find that the linear, second-order, third-order, and fourth-order IAHEs are supported by 31, 39, 15, and 4 3D MPGs, respectively, which means that one can observe Hall signal in almost all of \mathcal{T} -broken crystals (The leading contribution for linear and second-order IAHEs can be found in TABLE I of Supplemental Material²⁴, in which a full classification rather than leading order is also given.) It should be noted that the MPGs hosting linear/nonlinear IAHE, are/aren't compatible with ferromagnetism, therefore, the high-order Hall current response, as the leading contribution, can only be observed in AFM materials. We also note that the linear IAHE is normally assumed to be proportional to magnetization such as in FM metals, but theoretical predictions and experimental observations have recognized that large Hall effects can also occur in non-collinear or collinear AFM crystals^{35–38}, offered by neither of the global magnetic-dipole symmetry-breaking mechanisms^{39,40}. The symmetry arguments to search for the third-order IAHE in \mathcal{T} -broken systems, as the leading contribution, is our second main result.

Two-band model. — In this section, we employ a two-band model to illustrate our general theory. To that purpose, let us first consider the typical transport platform with planar geometry, in which the applied electric field \mathbf{E} and the generated current both within the plane (denoted as xy plane without loss of generality), and assuming the \mathbf{E} field forming an angle θ with the principal axis x of the crystal, namely $\mathbf{E} = E(\cos\theta, \sin\theta)$, we find that the in-plane intrinsic third-order anomalous Hall current density can be calculated as⁴¹:

$$J_{\text{AH}}^{(3)} = E^3 [\chi_{yxxx}^{\text{int}} \cos^2\theta - \chi_{xyyy}^{\text{int}} \sin^2\theta] + \frac{1}{2} E^3 \sin 2\theta [\chi_{xyxy}^{\text{int}} + \chi_{yxyx}^{\text{int}}] \quad (12)$$

Meanwhile, we note that the in-plane intrinsic third-order parallel current $J_{\parallel}^{(3)}$ is zero⁴¹. For simplicity, below we

will take $\theta = 0$ and hence $J_{\text{AH}}^{(3)} = \chi_{yxxx}^{\text{int}} E^3$.

Following the full classification in the Supplemental Material²⁴, the two-band model respecting MPG $4'm'm$

$$H(\mathbf{k}) = tk^2 + v(k_y\sigma_x - k_x\sigma_y) + m(k_x^2 - k_y^2)\sigma_z \quad (13)$$

is chosen to demonstrate the third-order IAHE, which is a low energy effective Hamiltonian to describe the band behavior around the Γ point of monolayer SrMnBi_2 ²³. In Eq.(13), σ_i ($i = x, y, z$) represent the Pauli matrices acting on the spin, and $k^2 = k_x^2 + k_y^2$. The band dispersion for this model is $\epsilon_{\pm} = tk^2 \pm h$ with $h^2 = v^2k^2 + m^2(k_x^2 - k_y^2)^2$ even in k_x and k_y , as shown in FIG.1(a), which resembles the Rashba dispersion but with a \mathcal{T} -broken second-order warping term²³. Interestingly, this effective model also has been utilized to demonstrate the existence of the third-order extrinsic anomalous Hall effect, as the leading contribution induced by Berry quadrupole²³.

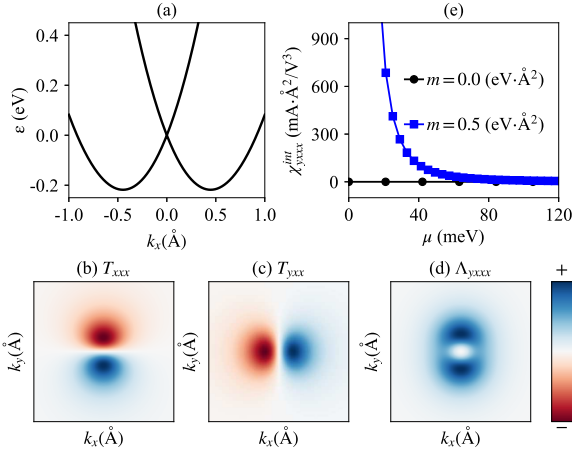


FIG. 1. (a) The band structure along k_x direction for the two-band model. (b-d) The \mathbf{k} -resolved distribution of T_{xxx} , T_{yxx} , and Λ_{yxxx} for the lower band of the two-band model. (e) The intrinsic third-order anomalous Hall conductivity χ_{yxxx}^{int} versus the chemical potential μ . Model parameters: $t = 1.2(\text{eV} \cdot \text{\AA}^2)$, $v = 1.0(\text{eV} \cdot \text{\AA})$, and $m = 0.5(\text{eV} \cdot \text{\AA}^2)$, which approximately describes the valence band edge of monolayer SrMnBi_2 around the Γ point²³.

For this model, the conventional BC for the lower band is found to be:

$$\Omega_z = -\frac{mv^2(k_x^2 - k_y^2)}{2\hbar^3} \quad (14)$$

which is even in k_x and k_y . However, due to the mirror symmetry \mathcal{M}_{x+y} , the integral for Ω_z in the Brillouin zone vanishes and hence there is no linear IAHE. Similarly, the first-order field-dependent BC for the lower band is given as:

$$\Omega_z^{(1)}/E_x = -\frac{v^2k_y[v^2 + m^2(3k_x^2 + k_y^2)]}{2\hbar^5} \quad (15)$$

which is odd in k_y and hence makes no contribution to IAHE at the second order. Note that this result is not

inconsistent with our full classification, in which the system with MPG $4'm'm$ can hold a leading-order second-order IAHE but involving an out-of-plane index, in which the nonvanishing components for the second-order IAHE conductivity tensor will be $\chi_{xzy}^{\text{int}} = \chi_{yzy}^{\text{int}} = -\chi_{zzy}^{\text{int}} = -\chi_{zzx}^{\text{int}}$. Here we focus on the third-order nonlinear transport behavior of this model. In terms of our third-order semiclassical theory, the second-order field-dependent BC for the lower band can be calculated as:

$$\Omega_z^{(2)}/E_x^2 = \partial_x T_{yxx} - \partial_y T_{xxx} = \frac{g_1 m^3 v^2 + g_2 m v^4}{8\hbar^7} \quad (16)$$

with T_{yxx}/xxx the second-order BPTs and $g_{1/2}$ even functions of k_x and k_y ⁴². Therefore, we conclude that the second-order field-dependent BC will lead to a nonzero third-order Hall current response. More intuitively, we present the \mathbf{k} -resolved distribution for T_{xxx} , T_{yxx} , and Λ_{yxxx} (same as the $\Omega_z^{(2)}/E_x^2$ for the lower band, as shown in FIG.1(b-d), which determine the final result of χ_{yxxx}^{int} . Particularly, we find that both T_{xxx} and T_{yxx} exhibit a dipole pattern in momentum space, respectively, and the resultant integrand Λ_{yxxx} approximately features a negative ellipse landscape around Γ point. In FIG. 1(e), we calculate the third-order IAHE conductivity χ_{yxxx}^{int} at zero temperature, as a function of the chemical potential ($\mu > 0$ is assumed), from which we conclude that the third-order response is nonzero and becomes significant when the chemical potential is close to zero energy, manifesting the fact that the third-order intrinsic conductivity is concentrated around the small-gap region¹⁵. As a check, we find the third-order IAHE conductivity χ_{yxxx}^{int} will disappear when $m = 0$, namely when the \mathcal{T} -symmetry is recovered, as can also be easily seen from the Eq.(16).

Interestingly, when the chemical potential μ is around the band crossing point, we find that the band dispersion can be approximated as $\epsilon_{\pm} = \pm vk$ and the second-order BPT can be approximated as $T_{xxx}^{\pm} = \pm 3mk_y/(8v^3k^5)$ and $T_{yxx}^{\pm} = \mp mk_x/(4v^3k^5)$, where \pm denote the conduction band and valence band, respectively, then the third-order IAHE conductivity at zero temperature can be analytically calculated as $\chi_{yxxx}^{\text{int}} = 5me^4/(32\pi\hbar|\mu|^3)^{43}$, which shows a cubic dependence on $|\mu|^{-1}$, consistent with our numerical results. Note that we have recovered e and \hbar in our final result. Particularly, when $\mu = 0.01$ (eV), we find that $\chi_{yxxx}^{\text{int}} \sim 10^3(\text{mA} \cdot \text{\AA}^2/\text{V}^3)$, which corresponds to a Hall voltage $\sim 0.001(\mu\text{V})$ by taking the electric field $\sim 10^4(\text{V/m})$ ²³, the resistance $\sim 10^3(\Omega)$ ²³ and the lateral size for Hall bar $\sim 100(\mu\text{m})$ ¹⁵. Although this Hall voltage is lower by an order of magnitude than the second-order intrinsic anomalous Hall voltage¹⁵, which can be detected experimentally.

Summary.— In this work, we develop the third-order semiclassical theory for Bloch electrons under the uniform external electric field with the semiclassical wavepacket approach. As one of the important applications, we predict that the third-order IAHE, driven by

the band geometric quantity—the second-order BC arising from the second-order field-induced *positional shift*, can occur in \mathcal{T} -broken systems. It should be emphasized that the third-order IAHE, as an important member of the nonlinear Hall family, has not been explored so far due to the lack of an appropriate theoretical approach. Furthermore, with symmetry arguments, we find that almost all the MPGs without time-reversal symmetry can be classified by linear, second-order, third-order, and also fourth-order IAHEs. Importantly, we find the intrinsic third-order nonlinear anomalous Hall signal, as the leading contribution, can be accommodated by 15 3D MPGs and hence fill the gap in previous studies, especially in AFM spintronics. Finally, a two-band toy model is employed to demonstrate the generalized theory.

Last but not least, we note that our third-order semi-

classical theory relies only on the properties of Bloch bands, which indicates that our theory can be combined with first-principles calculations to explore the IAHE of the realistic AFM materials. For example, following our symmetry analysis, the AFM materials MnTe^{44} and $\text{CoNb}_3\text{S}_6^{45}$ should exhibit a leading-order three-order IAHE signal, which will be explored in future works.

ACKNOWLEDGEMENTS

This work was financially supported by the Natural Science Foundation of China (Grant No.12034014 and No. 12004442) and Guangdong Basic and Applied Basic Research Foundation (Grants No. 2021B1515130007).

-
- * jianwang@hku.hk
- ¹ R. Karplus and J. M. Luttinger, Phys. Rev. 95, 1154 (1954).
 - ² N. Nagaosa, J. Sinova, S. Onoda, A. H. MacDonald, and N. P. Ong, Rev. Mod. Phys. 82, 1539 (2010).
 - ³ S. Murakami, N. Nagaosa, S.-C. Zhang, Science 301, 1348 (2003).
 - ⁴ J. Sinova, D. Culcer, Q. Niu, N. A. Sinitsyn, T. Jungwirth, and A. H. MacDonald, Phys. Rev. Lett. 92, 126603 (2004).
 - ⁵ E. Hall, American Journal of Mathematics 2, 287 (1879).
 - ⁶ L.D. Landau, E.M. Lifshitz and L.P. Pitaevskii, in *Statistical Physics*, Course of Theoretical Physics Vol. 5 3rd. ed. (Pergamon Press, Oxford, 1999)
 - ⁷ D. Xiao, M.-C. Chang, and Q. Niu, Rev. Mod. Phys. 82, 1959 (2010).
 - ⁸ I. Sodemann and L. Fu, Phys. Rev. Lett. 115, 216806 (2015).
 - ⁹ Q. Ma, S.-Y. Xu, H. Shen, D. MacNeill, V. Fatemi, T.-R. Chang, A.M.M. Valdivia, S. Wu, Z. Du, C.-H. Hsu, S. Fang, Q.D. Gibson, K. Watanabe, T. Taniguchi, R.J. Cava, E. Kaxiras, H.-Z. Lu, H. Lin, L. Fu, N. Gedik, and P. Jarillo-Herrero, Nature 565, 337 (2019).
 - ¹⁰ R. Battilomo, N. Scopigno, and C. Ortix, Phys. Rev. Lett. 123, 196403 (2019).
 - ¹¹ R. K. Malla, A. Saxena, and W. J. M. Kort-Kamp, Phys. Rev. B 104, 205422 (2021).
 - ¹² Z. Z. Du, H.-Z. Lu, and X. C. Xie, Nat. Rev. Phys. 3, 744 (2021).
 - ¹³ Y. Gao, S.A. Yang, and Q. Niu, Phys. Rev. Lett. 112, 166601 (2014).
 - ¹⁴ C. Wang, Y. Gao, and D. Xiao, Phys. Rev. Lett. 127, 277201 (2021).
 - ¹⁵ H. Liu, J. Zhao, Y.-X. Huang, W. Wu, X.-L. Sheng, C. Xiao, and S. A. Yang, Phys. Rev. Lett. 127, 277202 (2021).
 - ¹⁶ L.J. Xiang and J. Wang, arXiv:2209.03527.
 - ¹⁷ Y.-X. Huang, X.L. Feng, H. Wang, C. Xiao, and S.Y.A. Yang, arXiv:2208.03639.
 - ¹⁸ S. Lai, H. Liu, Z. Zhang, J. Zhao, X. Feng, N. Wang, C. Tang, Y. Liu, K. S. Novoselov, S. A. Yang, and W. B. Gao, Nat. Nanotechnol. 16, 869 (2021).
 - ¹⁹ C. Wang, R.-C. Xiao, H. Liu, Z. Zhang, S. Lai, C. Zhu, H. Cai, N. Wang, S. Chen, Y. Deng, Z. Liu, S.A. Yang, and W.-B. Gao, National Science Review nwac020, 2095 (2022).
 - ²⁰ T. Nag, S. K. Das, C.C. Zeng, S. Nandy, arXiv:2209.06867.
 - ²¹ X.-G. Ye, P.-F. Zhu, W.-Z. Xu, Z.H. Zang, Y. Ye, and Z.-M. Liao, Phys. Rev. B 106, 045414 (2022).
 - ²² H. Liu, J. Zhao, Y.-X. Huang, X. Feng, C. Xiao, W. Wu, S. Lai, W.-B. Gao, and S.A. Yang, Phys. Rev. B 105, 045118 (2022).
 - ²³ C.-P. Zhang, X.-J. Gao, Y.-M. Xie, H.C. Po, and K.T. Law, arXiv:2012.15628.
 - ²⁴ See Supplemental Material at [URL will be inserted by publisher] for the construction of wavepacket accurate up to the second order (see, also, references [3-4] therein), the derivation of second-order *positional shift*, the derivation of energy correction appeared in third-order semiclassical EOM, the full classification for \mathcal{T} -broken MPGs by AHE at different orders and the derivation of third-order anomalous Hall current density.
 - ²⁵ Y. Gao, S. A. Yang, and Q. Niu, Phys. Rev. B 91, 214405 (2015).
 - ²⁶ C. Xiao, H.Y. Liu, J.Z. Zhao, S.Y.A. Yang, and Q. Niu, Phys. Rev. B 103, 045401 (2021).
 - ²⁷ C. Xiao, H.Y. Liu, W.K. Wu, H. Wang, Q. Niu, and S.Y.A. Yang, Phys. Rev. Lett. 129, 086602 (2022).
 - ²⁸ Y. Gao, Low. Temp. Phys. Lett. 41, 0241 (2019).
 - ²⁹ Y. Gao, Frontiers of Physics 14, 1 (2019).
 - ³⁰ F. D. M. Haldane, Phys. Rev. Lett. 93, 206602 (2004).
 - ³¹ Neumann's principle can be stated as: if a crystal is invariant with respect to certain symmetry, any of its physical properties must also be invariant with respect to the same symmetry. As a consequence of this principle, symmetry imposes constraint on the physical quantity, making the relevant effect disappear.
 - ³² R. E. Newnham, Properties of Materials: Anisotropy, Symmetry, Structure (Oxford University Press, 2005).
 - ³³ H. A. Jahn, Acta Crystallogr. 2, 30 (1949).
 - ³⁴ S. V. Gallego, J. Etxebarria, L. Elcoro, E. S. Tasci, and J. M. Perez-Mato, Acta Crystallogr. Sect. A 75, 438 (2019).
 - ³⁵ H. Chen, Q. Niu, and A. H. MacDonald, Phys. Rev. Lett. 112, 017205 (2014).
 - ³⁶ C. Sürgers, G. Fischer, P. Winkel, and H. v. Löhneysen, Nat. Commun. 5, 3400 (2014).

- ³⁷ S. Nakatsuji, N. Kiyohara, and T. Higo, *Nature* 527, 212 (2015).
- ³⁸ T. Suzuki, R. Chisnell, A. Devarakonda, Y.-T. Liu, W. Feng, D. Xiao, J. W. Lynn, and J. G. Checkelsky, *Nat. Phys.* 12, 1119 (2016).
- ³⁹ L. Smejkal, R. Gonzalez-Hernandez, T. Jungwirth, and J. Sinova, *Sci. Adv.* 6, eaaz8809 (2020).
- ⁴⁰ L. Smejkal, A.H. MacDonald, J. Sinova, S. Nakatsuji, T. Jungwirth, *Nat. Rev. Mater.* 7, 482 (2022).
- ⁴¹ See section IV in the supporting materials for the details.
- ⁴² We have $T_{yxx} = k_x m v^2 / (4\hbar^5)$ and $T_{xxx} = -3k_y m v^2 / (8\hbar^5)$ from which we obtain $g_1 = -15k_x^4 + 40k_x^2 k_y^2 - 25k_y^4$ and $g_2 = -5k_x^2 - 10k_y^2$. Since g_2 is negative definite, its contribution to Eq.(16) is nonzero and hence the third-order IAHE is nonzero for this model.
- ⁴³ We note that the final result $\chi_{yxx}^{\text{int}} = 5me^4 / (32\pi\hbar|\mu|^3)$ diverges when the chemical potential μ lies exactly at the band crossing point, which may be regularized by disorder effect¹⁴.
- ⁴⁴ D. Kriegner, H. Reichlova, J. Grenzer, W. Schmidt, E. Ressouche, J. Godinho, T. Wagner, S. Y. Martin, A. B. Shick, V. V. Volobuev, G. Springholz, V. Holý, J. Wunderlich, T. Jungwirth, and K. Výborný, *Phys. Rev. B* 96, 214418 (2017).
- ⁴⁵ N.J. Ghimire, A.S. Botana, J.S. Jiang, J. Zhang, Y.-S. Chen, and J. F. Mitchell, *Nat. Commun.* 9, 3280 (2018).